Geochemistry Geophysics Geosystems G3
AN ELECTRONIC JOURNAL OF THE EARTH SCIENCES
Published by AGU and the Geochemical Society

Article
Volume 3, Number 11
29 November 2002
8504, doi:10.1029/2002GC000370
ISSN: 1525-2027

Wolf–Darwin lineament and plume–ridge interaction in northern Galápagos

Karen Harpp
Department of Geology, Colgate University, 13 Oak Drive, Hamilton, New York 13346, USA (kharpp@mail.colgate.edu)

Dennis Geist
Department of Geological Sciences, University of Idaho, Moscow, Idaho 83844, USA (dgeist@uidaho.edu)

[1] The Wolf–Darwin Lineament (WDL), located in the northwestern sector of the Galápagos Archipelago, lies between the focus of the Galápagos hot spot and the Galápagos Spreading Center. Consequently, most researchers have attributed its origin to the interaction between the plume and the adjacent ridge. We propose that the WDL is caused only partially by the plume–ridge interaction, and instead that it is primarily the result of tensional stresses emanating from the inside corner of the transform fault at 91°W. An additional factor that amplifies the tension in this region is the oblique orientation of the major transform fault with respect to the Nazca plate's spreading direction. This setting creates a transtensional zone whereby strain is partitioned into strike-slip motion along the transform and extension throughout the inside corner of the ridge–transform system. The area under tension is magmatic owing to the overlapping effects of the ridge and the Galápagos plume. The extensional model predicts no age-progressive volcanism, which is supported by observed age relationships. The WDL volcanoes define two distinct chemical groups: lavas erupted south of Wolf Island have compositions similar to those produced along the GSC west of 93°W, while those from the northern WDL resemble GSC lavas from the segment directly north of the lineament. This geographic distribution implies that the WDL is supplied by the same type of plume-affected mantle as the segment of the GSC that produced the lithosphere underlying the volcanoes. The observed WDL geochemical gradients are consistent with the extension model; the region under tension simply taps hybrid products of mixing at the margins of the subridge convection system and the periphery of the plume. Essentially, the stress field around the transform fault, normally not observable in a typical midocean ridge setting, is illuminated by the presence of melt from the adjacent hot spot.

Components: 8821 words, 8 figures.

Index Terms: 1025 Geochemistry: Composition of the mantle; 8121 Tectonophysics: Dynamics, convection currents and mantle plumes; 3035 Marine Geology and Geophysics: Midocean ridge processes.

Received 29 April 2002; **Revised** 13 August 2002; **Accepted** 27 August 2002; **Published** 29 November 2002.

Harpp, K., and D. Geist, Wolf–Darwin lineament and plume–ridge interaction in northern Galápagos, *Geochem. Geophys. Geosyst.*, *3*(11), 8504, doi:10.1029/2002GC000370, 2002.

Theme: Plume-Ridge Interaction **Guest Editor:** David Graham

1. Introduction

[2] The proximity of hot spots to ridge axes results in geomorphic and geochemical anomalies in both features, evidence of the exchange of material and heat between the systems [*Schilling*, 1991]. Plume–ridge interactions are at their most extreme at ridge-centered hot spots such as Iceland, but in that setting it can be difficult to distinguish plume-related activity from midocean ridge processes where the features are superimposed both spatially and temporally [e.g., *Fitton et al.*, 1997; *Wolfe et al.*, 1997] (B. B. Hanan et al., Depleted Iceland mantle plume geochemical signature; artifact of multicomponent mixing?, submitted to *Geochemistry, Geophysics, Geosystems*, 2000). In the Galápagos region, in contrast, the hot spot lies close to but not directly on the nearby plate boundary, and is between 150 and 250 km south of the Galápagos Spreading Center (GSC). The hot spot is thought to underlie the western islands of Fernandina and Isabela on the basis of the concentration of modern activity there as well as high $^{3}He/^{4}He$ ratios [*Graham et al.*, 1993; *Kurz and Geist*, 1999]. Consequently, the Galápagos region is one of the best locations in the world to study plume–ridge interactions, because the MOR and the plume are sufficiently close that they interact strongly with each other, yet sufficiently distant to remain distinct tectonic–magmatic systems.

[3] The focus of this study is the ocean floor between the main Galápagos Archipelago and the GSC. A group of enigmatic volcanoes populates the ocean floor between the hot spot and the GSC, including several isolated islands (Pinta, Marchena, and Genovesa) and one of the region's most notable features, the Wolf–Darwin Lineament (WDL), a NW–SE trending bathymetric high that connects the Galápagos platform to the GSC (Figure 1).

[4] Historically, the WDL has been treated as an integral part of the Galápagos hot spot. The wide variety of lava compositions and their complex spatial distribution along the lineament, however, have made it difficult to incorporate the WDL into existing models for the Galápagos plume [e.g., *White et al.*, 1993; *Harpp and White*, 2001]. The purpose of this paper is to review and reexamine observations bearing on the volcanic structures of the WDL and their relationship to both the Galápagos plume and to the adjacent midocean ridge.

[5] We propose that the Wolf–Darwin Lineament is not the direct result of hot spot activity, but instead the serendipitous product of the proximity of the plume to the major transform that offsets the GSC at 91°W. The adjacent plume and midocean ridge magmatic systems serve to generate widespread melting throughout the northern Galápagos region by causing upwelling in the mantle where it might not otherwise occur. The melts then migrate to the surface along tectonically controlled zones of tension imposed by an extensional transform. In effect, then, the adjacent plume "paints" the extensional zones with magma; at midocean ridge systems without a proximate plume, such zones are not rendered observable. The range of lava compositions erupted along the WDL reflects the heterogeneous nature of the underlying mantle and the complexity of plume–asthenosphere interaction throughout the region.

2. Wolf–Darwin Lineament: Background and Observations

2.1. Tectonic History of the Galápagos Region

[6] Plate motions in the Galápagos region have been complicated by migration of the ridge over the hot spot and plume–ridge interaction, as summarized by *Wilson and Hey* [1995]. Currently, the full spreading rate of the GSC at 91°W is approximately 56 km/my at 006°/186° (Nuvel-1A velocity of *DeMets et al.* [1994]; 58 km/my at 185° according to pole of *Wilson and Hey* [1995]). The motion of the Nazca plate relative to the global hot spot reference frame is 37 km/my at 91° [*Gripp and Gordon*, 1990]. The migration of a point on the ridge relative to the Galápagos hot spot is 47 km/my at 55°, the vector difference between the absolute motion of the Nazca plate and the GSC half-spreading velocity (Figure 2a). Obviously, the

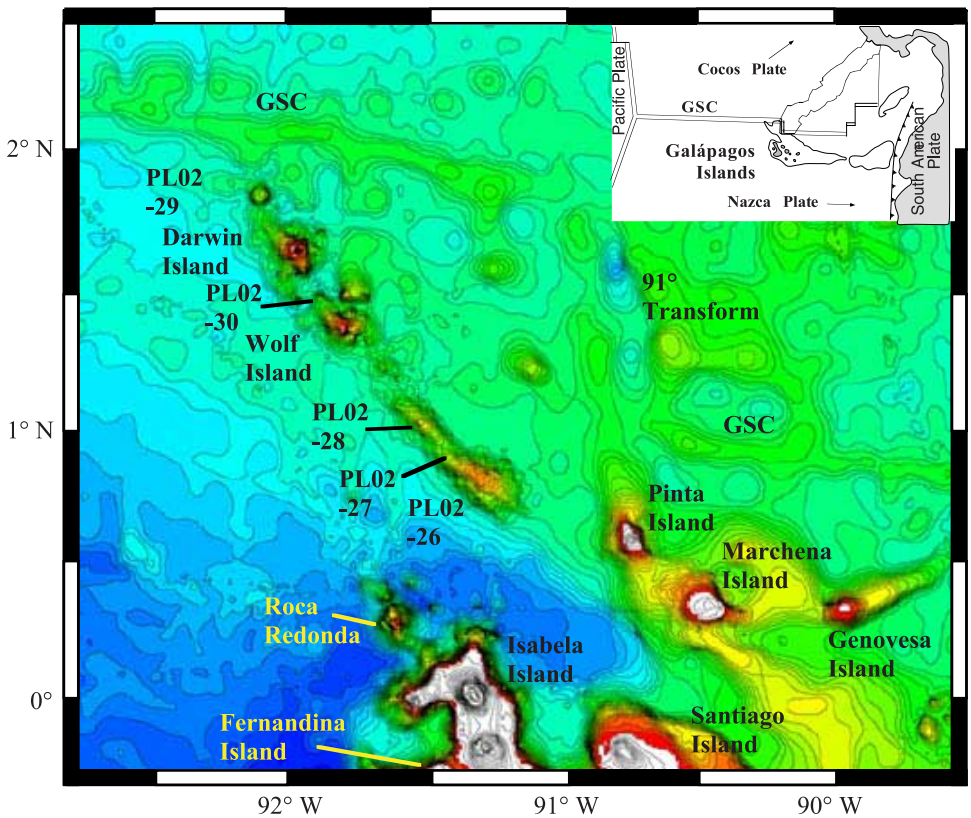

Figure 1. Bathymetric map of the northern Galápagos region, as compiled by Dr. William Chadwick of NOAA and Oregon State University and available at http://newport.pmel.noaa.gov/~chadwick/galapagos.html. Seamounts are labeled according to the dredge station from the PLUME02 cruise [*Christie et al.*, 1992].

trend of the WDL (140°) is strongly oblique to all of these motions.

[7] The absolute motion of the GSC and the 250 km separation between the ridge and Fernandina indicate the ridge may have overlain the plume until about 9 Ma, although studies of seafloor magnetics by *Wilson and Hey* [1995] suggest that this event occurred at 6 Ma. According to *Wilson and Hey*'s [1995] tectonic reconstructions, the Galápagos Spreading Center has undergone numerous jumps and reconfigurations throughout the past 10 Ma. In particular, the 91°W transform fault formed as a result of a southward ridge jump only about 3 Ma [*Wilson and Hey*, 1995].

2.2. Bathymetry

[8] The Wolf–Darwin Lineament is a bathymetric feature that trends 140° and includes Wolf and Darwin Islands (at latitudes 1.3°N and 1.7°N), several seamounts (1.9°N, 1.6°N, and 1.0°N), and an unusually elongate seamount that parallels the main trend of the WDL (from 0.8°N to 0.9°N; Figure 1). A pseudofault formed by the propagating ridge tip at 93°W crosses the WDL at about 1.5°N, meeting the lineament in the vicinity of the seamount between Wolf and Darwin Islands (site of sample PL02-30 [*Wilson and Hey*, 1995]). The pseudofault marks a discontinuity in lithospheric age; north of the boundary, the lithosphere is younger, having been produced east of 93°W on the GSC. Lithosphere underlying the southern WDL, in contrast, was erupted west of 93°W and is approximately one million years older than the northern WDL [*Wilson and Hey*, 1995]. The intersection of the pseudofault with the WDL does not appear to produce any bathymetric expression along the WDL (Figure 1).

[9] The WDL and the Galápagos Spreading Center meet at approximately 92.2°W, significantly west of

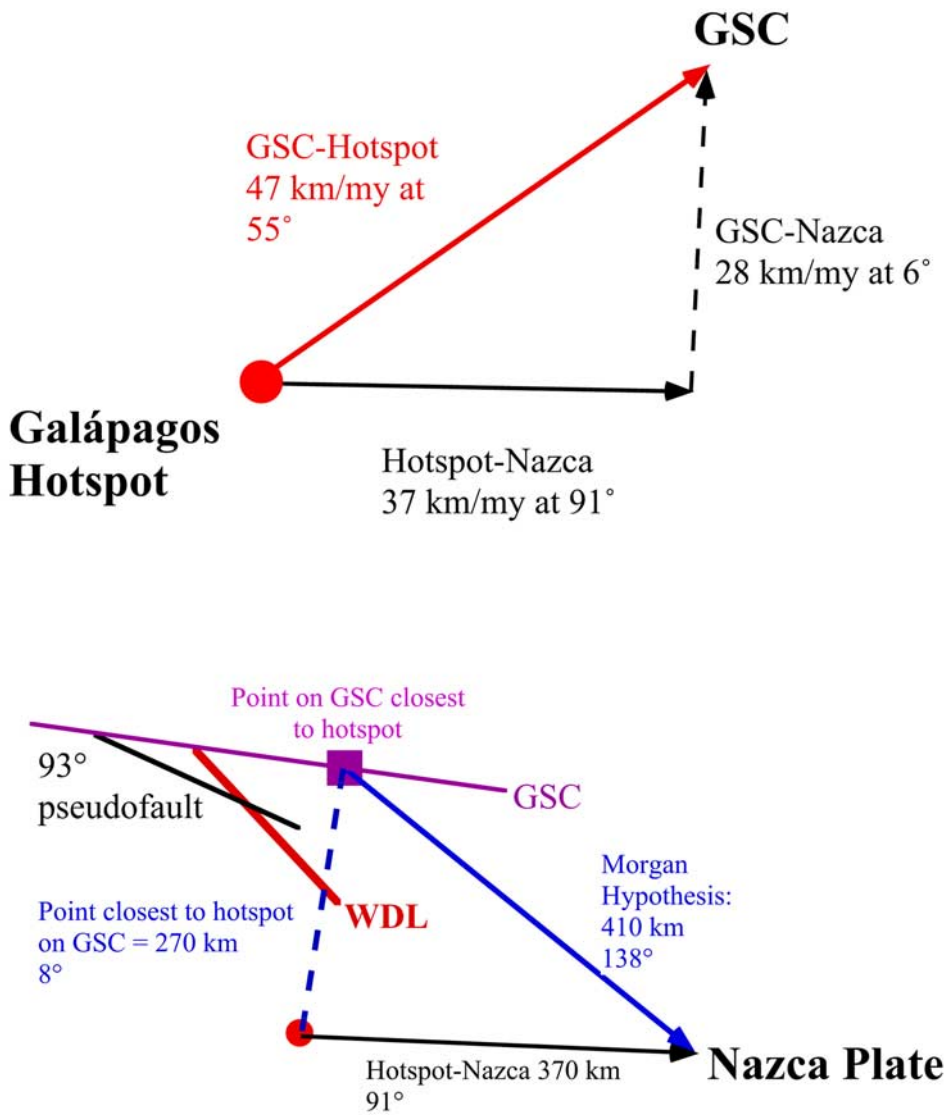

Figure 2. TOP: Tectonic motions in the Galápagos region, in velocity space. GSC-Nazca plate velocity (dashed black line) is half-spreading rate from *DeMets et al.* [1994]; Galápagos hotspot-Nazca plate velocity (solid black line) is calculated from pole of *Gripp and Gordon* [1990]. The movement of a point on the GSC relative to the Galápagos hotspot is the difference between these two vectors (solid red arrow; GSC-Galápagos hotspot). BOTTOM: Spatial orientation of lineaments in northern Galápagos compared to *Morgan* [1978] hypothesis for WDL. Note that this is not velocity space but absolute space; vectors show motions over 10 m.y. GSC (solid purple line) and WDL (solid red line) are determined from the bathymetric chart (Figure 1); orientation of the pseudofault from 93°W (dashed black line) on the GSC is from *Wilson and Hey* [1995]. The point on the GSC closest to the hotspot (current location indicated by the purple square) is located where the ridge intersects the perpendicular to the GSC that passes through the hotspot. Subtraction of the closest GSC point-hotspot vector (dashed blue line) from the movement of the Nazca plate relative to the hotspot (solid black) yields the alignment of seamounts predicted using *Morgan*'s [1978] hypothesis (solid black line).

Fernandina Island (91.5°W). The GSC shallows eastward to <2000 m from a base level of >2500 m at 94°W across the region from 94°W to 90.5°W, deepening again eastward to 88°W. Note that the local bathymetric high along the GSC is actually 20 km east of the WDL–GSC intersection, which marks the peak of a broad bathymetric swell on the ridge between approximately 93° and 88°W (Figure

1) [e.g., *Schilling et al.*, 1976; *Canales et al.*, 1997]. Additional seamounts populate the region between the WDL and the 91°W transform, but they do not form as prominent a set of lineaments as the WDL.

[10] Whereas Pinta and Marchena could be viewed as an offset, southern extension of the WDL, a wide expanse of >2000 m deep water separates the elongate seamount at 0.8°N on the WDL from Pinta Island (Figure 1). We therefore treat the WDL as a distinct feature that terminates at the southernmost seamount (PL02-26; Figure 1).

[11] The volcanoes of the WDL occupy a region of the ocean floor that is topographically distinct from the main Galápagos Archipelago. A broad deep reaching to over 3000 m separates northern Isabela and Roca Redonda volcano from the WDL. Clearly, the WDL does not connect the most volcanically active part of the Galápagos (Isabela and Fernandina islands) with the GSC. Instead, the WDL points toward the eastern (older) part of the Galápagos platform, which was most active over 2 million years ago [*Geist et al.*, 1986].

2.3. Chronology

[12] Lithospheric ages determined by magnetic anomalies provide an upper limit for the formation of the northern volcanoes. The lithosphere ranges from effectively zero-age at the seamount north of Darwin Island (PL02-29) to a maximum of ~7 Ma at the southern extent of the WDL [*Wilson and Hey*, 1995]. North of Wolf Island, the pseudofault that extends from 93°W crosses the WDL, resulting in an abrupt increase (~1 million years) in lithospheric ages for the southern half of the Wolf–Darwin Lineament [*Wilson and Hey*, 1995].

[13] All of the volcanoes and seamounts of the WDL are young, ranging from essentially zero age to 1.60 ± 0.07 Ma at Wolf Island [*White et al.*, 1993] and 1.7 ± 0.1 Ma at the seamount north of Wolf (Figure 3) (PL02-30; plateau age of *Sinton et al.* [1996]). The WDL volcanoes are thus all considerably younger than the underlying lithosphere and could not have formed near the ridge as anticipated by *Morgan* [1978]. Also, as noted by *Sinton et al.* [1996], the ages of the islands and seamounts do not correlate with distance from the hot spot's focus, distance from the GSC, or any geochemical parameter. The only apparent pattern is that ages generally decrease away from Wolf Island along the lineament.

2.4. Volcano Morphology

[14] Wolf and Darwin Islands are small compared to the large shields of the western archipelago, even when the submarine parts of the northern volcanoes are considered. In fact, they are comparable in volume to near-ridge seamounts (calculated from their submarine base; e.g., *Allan et al.* [1989]). The islands are emergent in part because the seafloor produced by the GSC in this region is anomalously shallow, owing to plume–ridge interaction. In addition, Wolf and Darwin Islands do not have the characteristic Galápagos "soup bowl" morphology of the western volcanoes [*McBirney and Williams*, 1969]. Instead, they appear to be the wave-eroded emergent tops of volcanoes, similar to Roca Redonda's steep-sided structure [*Standish et al.*, 1998].

[15] One of the unique characteristics of the WDL volcanoes is that some of them deviate from the typical, symmetrical structures of most seamounts and many ocean islands. The southernmost seamounts of the WDL, as well as Wolf and Darwin volcanoes, are unusually elongate edifices that trend parallel to the overall strike of their local lineament, with multiple constructional peaks [*Christie and Fox*, 1990]. The seafloor between Pinta and Marchena is also cut by fractures and fissures parallel to the WDL [*Fornari et al.*, 2001]; similar fissures are observed in the vicinity of Genovesa Island, but with a northeastward strike [*Harpp et al.*, 2002]. Elongate seamounts are unusual features in off-axis seamount provinces [*Batiza and Vanko*, 1983; *Smith and Cann*, 1992], and are indicative of unusually strong deviatoric stresses on a regional scale.

2.5. Lithologies and Compositions

[16] One of the petrologic features that distinguishes the northern lavas from those of the main Galápagos Archipelago is the abundance of plagioclase-ultraphyric basalts. These lavas contain up

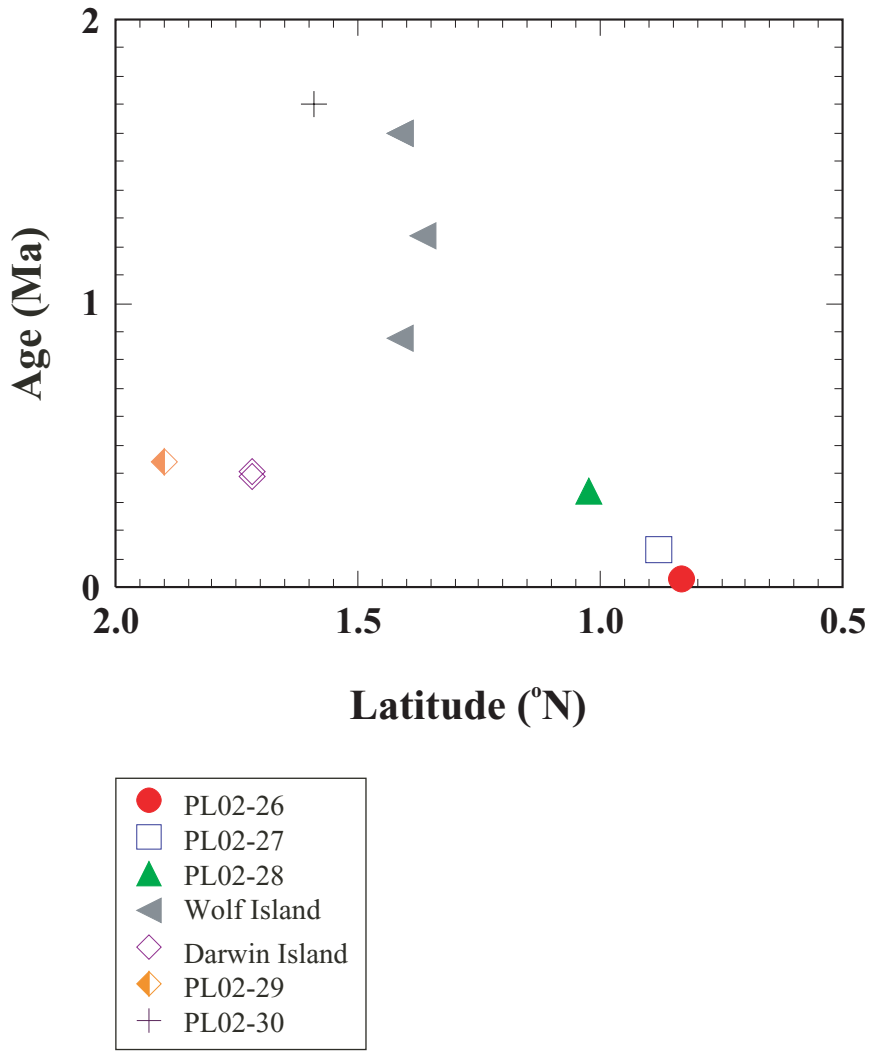

Figure 3. Variation in ages of WDL volcanoes with latitude. Data compiled from *White et al.* [1993] and *Sinton et al.* [1996].

to 50% anorthitic plagioclase megacrysts that can reach 3 cm in length [*Cullen et al.*, 1989; *Vicenzi et al.*, 1990; *Harpp et al.*, 2002; *Sinton et al.*, 1993]. Every island in the northern region has erupted these lavas, whereas they are rare in the main archipelago [*Cullen et al.*, 1989]. The seamounts of the WDL have also produced plagioclase-phyric lavas, although phenocryst sizes are not as large as those observed on the islands.

[17] The trace element and isotopic characteristics of basalts from the WDL exhibit a wide diversity of compositions, almost encompassing the range of the entire archipelago (Figure 4) [e.g., *Harpp and White*, 2001]. In contrast, helium isotopes possess more uniform values, from 6.9 to 8.8 R_a, lower than most Galápagos Archipelago lavas but close to normal MORB values [*Graham et al.*, 1993]. Rare earth element (REE) patterns for the WDL volcanoes vary from light rare earth element-enriched (LREE; e.g., Darwin Island and PL02-30) to LREE-depleted patterns indistinguishable from MORB (e.g., PL02-26; Figures 5 and 6). Trace element abundances and ratios of highly incompatible to moderately incompatible elements generally correlate with isotopic signatures [*White et al.*, 1993; *Harpp and White*, 2001], but the correlation is imperfect. Interestingly, most of the WDL lavas exhibit higher Sm/Yb ratios than are observed in lavas erupted along the GSC axis at the same longitude, except for PL02-

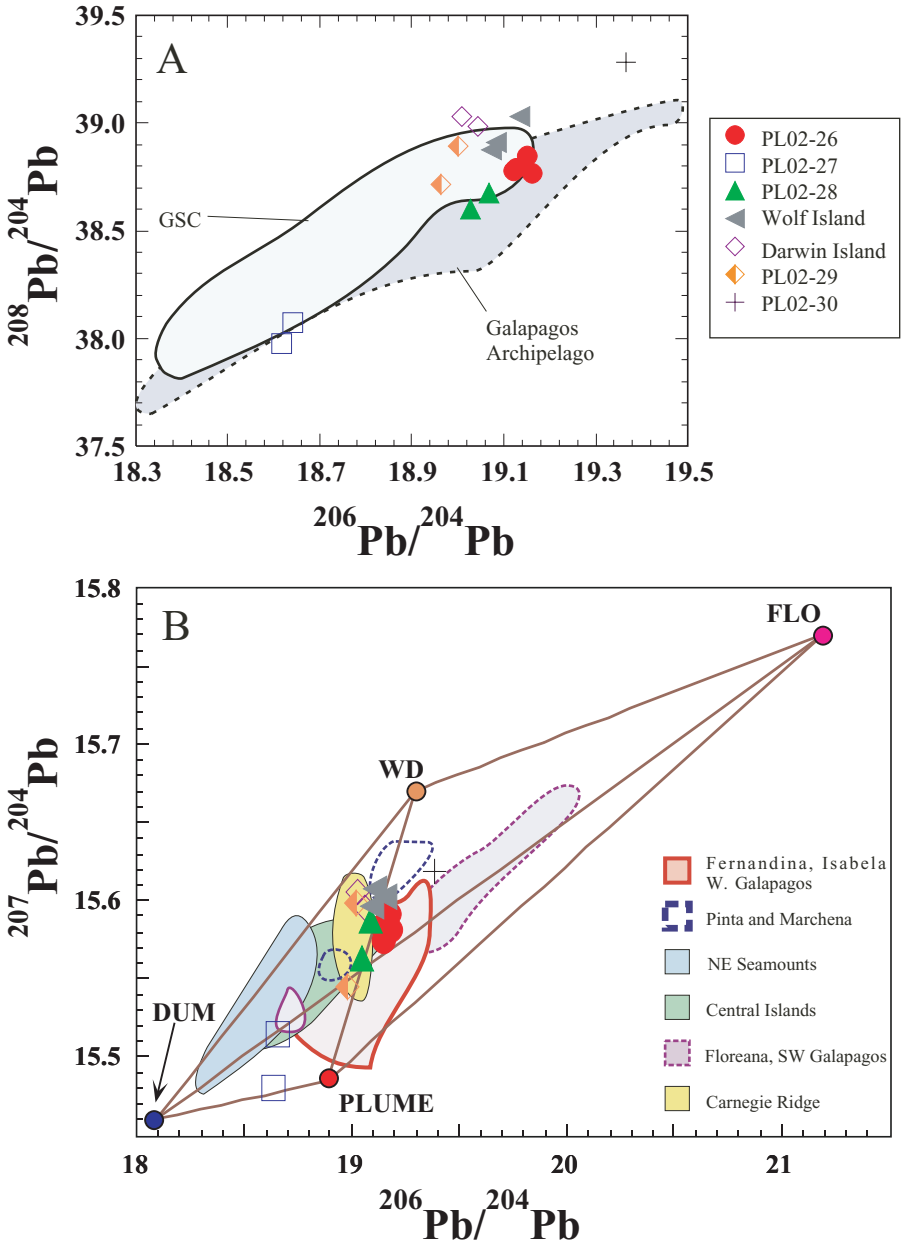

Figure 4. Lead isotopic ratios of northern Galápagos volcanoes. Data for Darwin, Wolf, Pinta, and Marchena islands from *White et al.* [1993]; Wolf and PL02 data from *Harpp and White* [2001]; Genovesa Island data from *Harpp et al.* [2002]. A. Detailed view of $^{208}Pb/^{204}Pb$ versus $^{206}Pb/^{204}Pb$. Grey field contains all Galápagos island and seamount data [*White et al.*, 1993; *Kurz and Geist*, 1999; *Harpp and White*, 2001]. B. Mantle endmembers proposed by *Harpp and White* [2001] in $^{207}Pb/^{204}Pb$ versus $^{206}Pb/^{204}Pb$ space. Mixing lines shown in brown, endmembers as solid circles labeled DUM (depleted mantle), PLUME (Galápagos plume), WD (mantle component focused near WDL), and FLO (incompatible trace element enriched component centered in SW archipelago).

29, the seamount closest to the ridge (Figure 6) [e.g., *Schilling et al.*, 1982].

2.6. Spatial Patterns

[18] Most of the isotopic and trace element compositions of lavas from WDL volcanoes bear no simple relationship to their position along the strike of the lineament (Figure 7). Instead, geochemical parameters exhibit complex, and perhaps random, distributions along the WDL. For instance, $Na_2O + K_2O$ values are lowest at the intersection of the WDL and the GSC (PL02-29) and higher but essentially con-

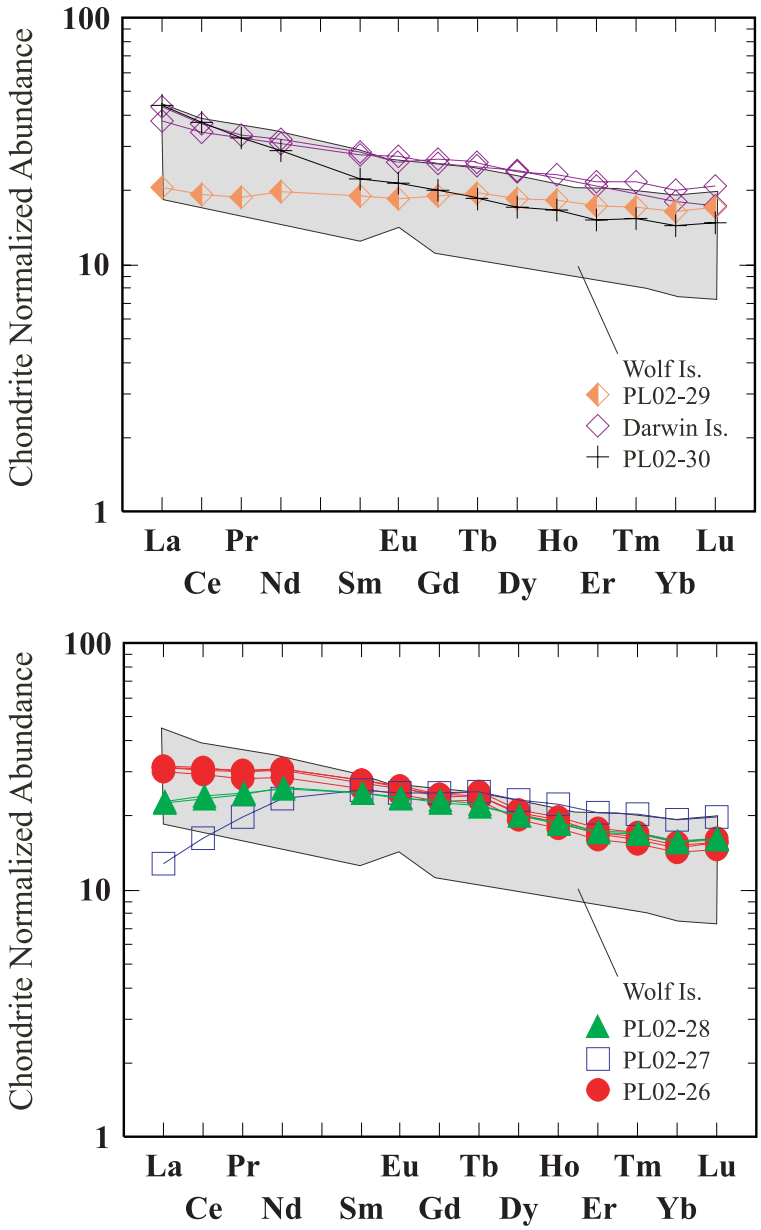

Figure 5. Representative REE plots. Data sources as in Figure 4. Chondrite normalization values from *McDonough and Sun* [1995].

stant in all of the volcanoes to the southeast. In contrast, Sm/Yb ratios generally increase to the southeast away from the GSC (Figure 7).

[19] Broadly, however, the WDL volcanoes can be divided into two distinct groups on the basis of their compositional variations along the lineament: a) the northern group (I), which extends from the GSC to Wolf Island and includes both of the islands as well as seamounts PL02-29 and 30; and b) the southern group (II), made up of the two southernmost seamounts (PL02-26 through 28). Group I lavas exhibit more enriched Sr and Nd (but not Pb) isotopic signatures (Figure 7) and elevated TiO_2, K_2O, Ba/La, La/Ce, and La/Sm compared to Group II volcanoes. Furthermore, *Graham et al.* [1993] noted that $^3He/^4He$ ratios are lower along the northern WDL (Group I) than they are in the southern half of the lineament (Figure 7). Finally, Group I lavas reveal an intriguing yet subtle difference in Pb isotopic ratios and in REE contents. At a given $^{206}Pb/^{204}Pb$, Group I

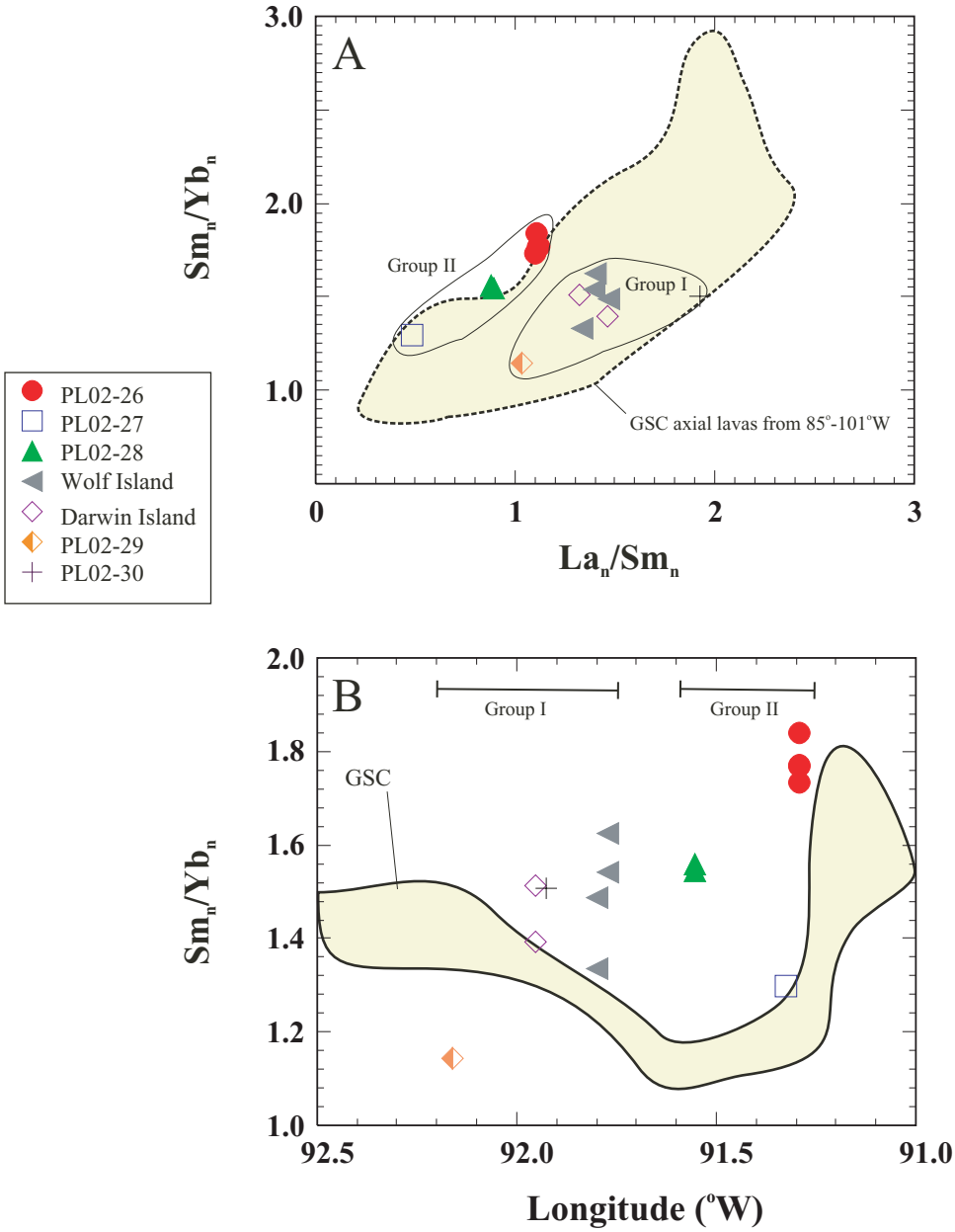

Figure 6. A. Sm_n/Yb_n versus La_n/Sm_n for the northern Galápagos volcanoes and GSC; B. Sm_n/Yb_n versus longitude for the Wolf–Darwin Lineament; field represents GSC axial lavas. Data sources as in Figure 4; GSC data from *Schilling et al.* [1982]. Chondrite normalization values from *McDonough and Sun* [1995].

lavas possess a higher $^{208}Pb/^{204}Pb$ ratio than lavas erupted at Group II volcanoes (Figure 4). Groups I and II define distinct trends on a REE ratio plot; Group II lavas have higher La/Sm for the same Sm/Yb compared to Group I (Figure 6).

2.7. WDL and the GSC

[20] Geochemical evidence indicates that the Galápagos hot spot is sufficiently close to the GSC to interact extensively with the ridge [e.g., *Schilling et al.*, 1982; *Detrick et al.*, 2002]. Lavas erupted at the GSC axis become progressively enriched as the ridge approaches the hot spot, consistent with interactions observed at other plume–ridge systems around the world [e.g., *Haase and Devey*, 1996; *Yu et al.*, 1997].

[21] Contrary to some of the early interpretations, lavas erupted along the GSC exhibit maximum

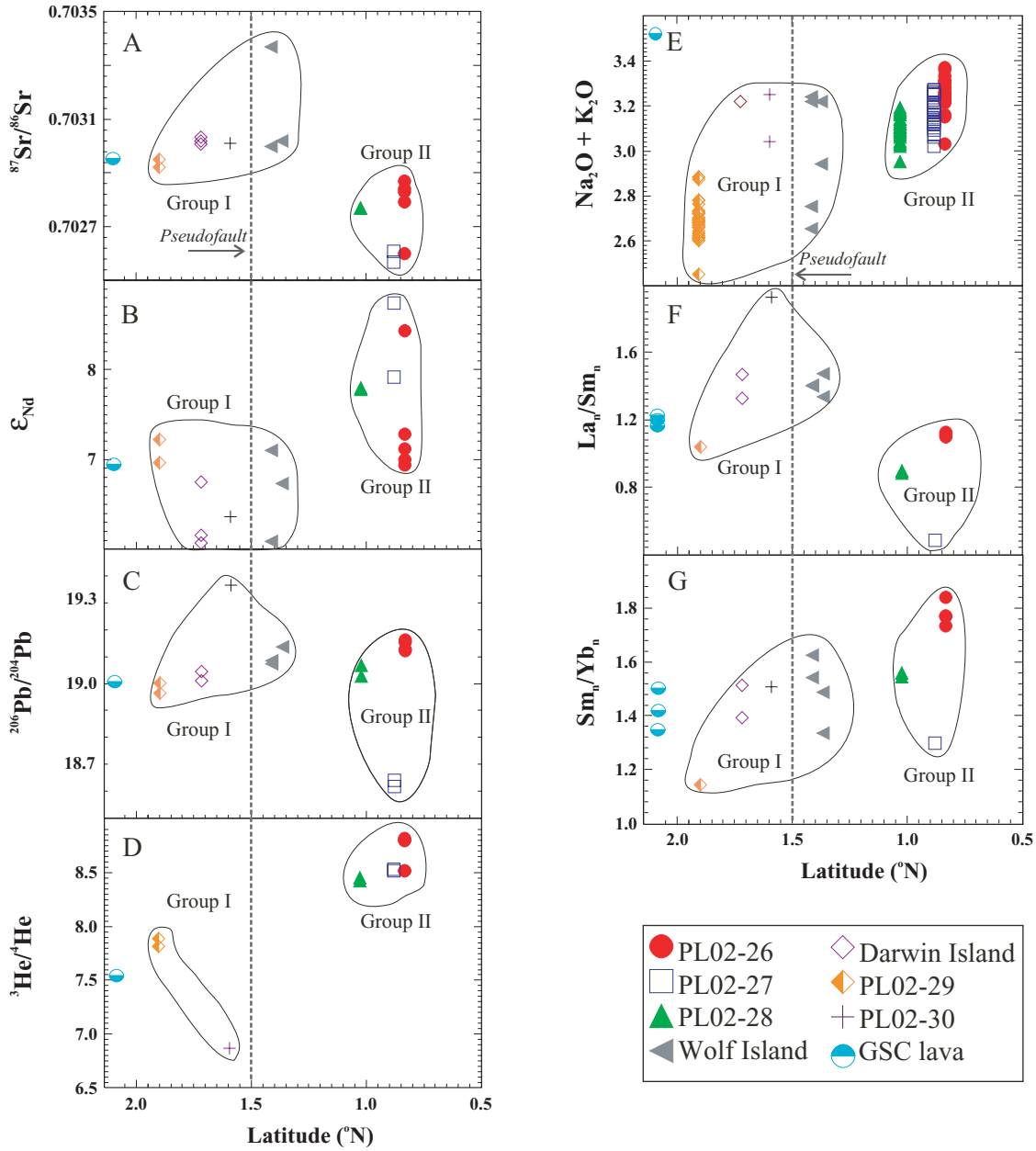

Figure 7. Geochemical variations along the Wolf–Darwin Lineament versus latitude. A. $^{87}Sr/^{86}Sr$; B. ε_{Nd}; C. $^{206}Pb/^{204}Pb$; D. $^{3}He/^{4}He$ R_A; E. $Na_2O + K_2O$; F. La_n/Sm_n; G. Sm_n/Yb_n. Data from *White et al.* [1993], *Harpp and White* [2001], and *Detrick et al.* [2002]. See text for definitions of Groups I and II. Grey dashed line marks the intersection of the 93°W pseudofault and the WDL [*Wilson and Hey*, 1995]. Only the point where the pseudofault intersects the WDL is indicated in the figure; the width of the area affected by the pseudofault may, however, be considerably greater. Chondrite normalization values from *McDonough and Sun* [1995].

geochemical enrichment not at a single point along the axis, but instead across a wide region of the ridge from 89°W to 95.5°W [cf. *Schilling et al.*, 1982; *Verma and Schilling*, 1982; *Verma et al.*, 1983] [*Detrick et al.*, 2002]. The WDL intersects the ridge at 92.2°W, within the most strongly plume-affected portion of the GSC on a regional scale, but not necessarily at the peak of enrichment. Recently, fine-scale sampling of the GSC west of the 91°W transform has been undertaken by *Detrick et al.* [2002]. Preliminary results suggest that at the intersection of the WDL and the GSC, there is no

dis-continuity in the regional geochemical gradients, including K/Ti, Nb/Zr, and $^{3}He/^{4}He$, although additional samples remain to be analyzed [*Detrick et al.*, 2002].

[22] The intersection of the WDL and the GSC at 92.2° coincides with a regional low in the residual mantle Bouger anomaly, interpreted as buoyant mantle beneath that part of the GSC [*Canales et al.*, 2002]. The buoyancy may be the result of the presence of melt in the shallow mantle or mantle made buoyant by partial melt extraction [*Canales et al.*, 2002]. In addition, preliminary results from an archipelago-wide seismic tomography experiment [*Toomey et al.*, 2001] show a narrow low velocity zone in the upper mantle that extends from deep below the western archipelago toward the shallow mantle beneath the WDL.

[23] Lavas from the northern part of the WDL (Group I) exhibit geochemical signatures virtually indistinguishable from those erupted along the GSC at comparable longitudes (Figure 6). In contrast, lavas from Group II, south of Wolf Island, are consistently more depleted than lavas produced at the axis directly to their north. The only notable exception is observed in $^{206}Pb/^{204}Pb$ variations, wherein only seamount PL02-27 is more depleted than GSC lavas at the same longitude.

2.8. Extent of Plume Contribution to the WDL Lavas

[24] In a statistical analysis of regional Galápagos lava compositions, *Harpp and White* [2001] propose that the isotopic and trace element variations observed throughout the archipelago (Figure 4) are the result of interaction among four mantle source reservoirs with distinct compositions: a) a mantle plume with typically enriched signatures (''PLUME''); b) the depleted upper mantle ("DUM"); c) an incompatible element-enriched, possibly metasomatically altered reservoir ("FLO"); and d) a fourth component distinct primarily in its lead isotope ratios (''WD''). Contributions from the four end-members exhibit a systematic geographic distribution. PLUME's influence is strongest in the western Galápagos, with increasing dilution by the depleted mantle (DUM) to the east, north, and south, away from the presumed hot spot center. FLO is localized in the SW archipelago and does not play a significant role in northern archipelago compositions. In contrast, WD is most prevalent in lavas from the Wolf–Darwin Lineament.

[25] In the context of the mantle end-members, WDL magmas are best described as hybrids between PLUME and WD, with minor contributions from DUM (Figure 4). Geochemical differences between Group I and II lavas suggest that Group I lavas (northern WDL) may be derived from sources with slightly more PLUME than those erupted along the southern WDL (Group II). This observation suggests that if Group I lavas are the result of a greater plume contribution than Group II, they must have experienced a melting event that caused the loss of the helium plume signature because $^{3}He/^{4}He$ ratios are lower in Group I than in Group II lavas [*Graham et al.*, 1993].

3. Discussion

[26] The most perplexing aspect of the WDL is that it does not lie in a direction that is logically related to any known tectonic features. It is oblique to the absolute motion of the Nazca plate (91° [*Gripp and Gordon*, 1990]), oblique to the motion of the Nazca plate relative to the GSC (186° [*Wilson and Hey*, 1995]), oblique to the difference between these two vectors (55°), and it is apparently unaffected by the pseudofault created by the 93°W propagating rift (Figure 2) [*Wilson and Hey*, 1995]. The existing paradigm is that the WDL lies above a mantle "pipeline" that channels plume material from the Galápagos hot spot to the GSC [e.g., *Morgan*, 1978]. We believe that most of the evidence contradicts such a model, and instead propose that the WDL is a zone of extension caused by strain partitioning and the tensional stresses set up in the ''inside corner'' of a ridge–transform intersection.

3.1. Pipeline Hypothesis

[27] The WDL has been interpreted as the surficial expression of a sublithospheric channel that connects the Galápagos plume to the GSC [e.g., *Verma*

et al., 1983]. Elsewhere on the planet, constructional ridges extend from near-ridge hot spots to adjacent spreading axes [*Small*, 1995]. One of the best examples of this phenomenon is the Easter hot spot, which is located about 350 km from the East Pacific Rise. There, a group of seamounts lies between the hot spot at Easter Island and the ridge [*Haase et al.*, 1997; *Rappaport et al.*, 1997; *Kingsley et al.*, 1998]. The seamount chain displays a gradient in isotopic signatures along strike wherein the maximum plume contribution occurs at Easter or Sala y Gomez Island and decreases regularly toward the EPR [*Haase et al.*, 1996; *Haase and Devey*, 1996; *Hanan and Schilling*, 1989]. The distribution of geochemical compositions is consistent with a model in which the seamounts erupt directly above a mantle pipeline connecting the hot spot with the ridge and reflect ongoing, progressive mixing between the plume source and the depleted mantle [e.g., *Haase et al.*, 1996].

[28] In contrast to observations along the Easter seamount chain [*Haase et al.*, 1996; *Hanan and Schilling*, 1989], source compositions along the WDL do not become progressively depleted closer to the GSC (Figure 7). Instead, they broadly exhibit the opposite trend, with the most depleted signatures occurring at the SE end of the lineament, farthest from the GSC. Furthermore, as described previously, the southern end of the WDL is hundreds of kilometers from the presumed plume center [e.g., *Kurz and Geist*, 1999].

[29] In a similar hypothesis, *Morgan* [1978] proposed that the WDL is the result of plume–ridge interaction complicated by the migration of the GSC relative to the plume. In this model, the Galápagos hot spot supplies material to the closest point on the GSC, generating volcanic centers at the ridge instead of erupting nearly contemporaneously over the channel. As the ridge migrates away from the hot spot, new volcanic centers are created at the axis and old volcanoes are carried away from the ridge by plate motion. Over time, this process eventually produces a linear feature such as the WDL. As noted by *Morgan* [1978], this hypothesis requires that the hot spot be over 100 km to the west of Fernandina, an area for which there is no evidence of recent volcanism [*Fornari et al.*, 2001] or the plume [*Toomey et al.*, 2001].

[30] There are a number of predictable outcomes of the Morgan model: 1) evidence of plume contribution to axial GSC lavas should be most pronounced at the intersection of the WDL with the ridge at 92.2°W; 2) the WDL should be aligned along a trend parallel to the vector difference between the northward component of the absolute motion of the GSC and the absolute motion of the Nazca plate (Figure 2) (41 km/my at 138° [*Morgan*, 1978; *Wilson and Hey*, 1995]); 3) the age of volcanism should increase from the GSC southeast along the WDL as seamounts produced at the ridge migrate away with plate motion; and 4) each volcanic center along the WDL should be the same age as its underlying lithosphere, both having been produced at or near the GSC.

[31] Whereas geochemical anomalies along the GSC reflect increasing plume contribution to the MOR source as the ridge approaches the hot spot, the maximum enrichment occurs over a broad section of the axis between approximately 90°W and 92°W [*Schilling et al.*, 1982; *Verma and Schilling*, 1982; *Verma et al.*, 1983; *Detrick et al.*, 2002], not at the intersection of the WDL with the GSC. The morphological evidence for plume interaction with the ridge, including inflated axial cross-section profiles and shallow bathymetry, confirm the geochemical observation that the GSC–WDL intersection may not mark the locus of maximum plume contribution to the ridge [*Canales et al.*, 1997], contrary to where the Easter seamount chain intersects the EPR [*Haase et al.*, 1996].

[32] In the *Morgan* [1978] hypothesis, the point of active seamount production on the ridge should be migrating about 27 km/my at 8° relative to the hot spot, and the seamount track on the Nazca plate should be oriented at 138°. The azimuth of the WDL does match that predicted by *Morgan* [1978]. Nevertheless, the hypothesis also explicitly predicts both an age progression along the WDL (41 km/my; Figure 2B) as well as correspondence between the volcano ages and those of the underlying litho-

sphere. *Sinton et al.* [1996] and *White et al.* [1993] noted that the volcanoes of the WDL do not exhibit any systematic age progression along strike and, moreover, are millions of years younger than the lithosphere on which they are constructed [*Wilson and Hey*, 1995].

[33] A modification of Morgan's hypothesis was proposed by *Small* [1995]. For many near-ridge hot spots, the topographic high always occurs at the midsegment along the ridge, approximately halfway between large-offset transforms, not at the point on the ridge closest to the hot spot. *Small* [1995] attributed this observation to differences in the thickness of the lithosphere, which should be greatest near the cold-edge of a transform and thinnest midsegment. If plume material buoyantly flows along the base of the lithosphere, it should migrate from the plume center up to the middle of the closest MOR segment, creating the observed topographic high along the ridge. At first glance, this explanation is an appealing one for the WDL, because its intersection with the GSC at 92.2°W is midway between the offset at 91°W and the propagator at 93°W (Figure 1). Upon closer inspection, however, the WDL does not emanate from the focus of the hot spot at Fernandina but from the eastern part of the Galápagos platform at approximately 90°W. Furthermore, the 93°W propagator only marks a small offset along the Galápagos Spreading Center, and in fact there are many smaller-scale offsets between the propagating rift and the transform [*Detrick et al.*, 2002]. Consequently, the discontinuity in lithospheric thickness due to cold-edge effects should be negligible there, eliminating the focusing effect toward the intersection of the WDL with the GSC.

3.2. WDL as a Result of an Extensional Transform Zone

[34] We propose that the Wolf–Darwin Lineament is the surface manifestation of transtensional stresses caused by plate motion around the 91°W transform fault (Figure 8). The obliquity of the transform induces extension throughout the region bounded by the 91°W transform fault in the east and the Wolf–Darwin Lineament in the west. Volcanoes are produced from the combination of unusually large deviatoric stresses imposed on the lithosphere coupled with excess magma production from plume–ridge interaction. Excess melt is generated in the mantle owing to the proximity of the Galápagos plume; the magma is able to ascend because of abnormal stresses throughout the region, causing constructional volcanism in atypical settings. In essence, the stress field around the transform fault, normally not observable in a typical midocean ridge setting, is illuminated by the presence of melt from the adjacent hot spot.

[35] Two-dimensional anisotropic finite element models of the stresses developed in the vicinity of a ridge–transform intersection suggest that large deviatoric stresses occur in the "inside corner" region of the intersection, and that tensional horizontal stress occurs in a direction that bisects the ridge–transform intersection [*Fujita and Sleep*, 1978]. In a two-dimensional boundary element model, *Gudmundsson* [1995] also showed that extension is induced within the inside corner of the intersection of a ridge with a large transform fault, precisely along the orientation of the WDL. Furthermore, *Gudmundsson*'s [1995] model predicts tensional stresses should be present throughout the region bounded by the ridge and the transform fault, providing an explanation for the smaller seamounts between the WDL and the 91°W transform (Figure 1). Similar stress regimes were obtained by boundary element models of the stresses in the inside corner of "underlapped" spreading centers [*Pollard and Aydin*, 1984].

[36] In addition, the stresses imparted on the Nazca plate by the transform fault may be enhanced because the transform is not parallel to the spreading direction. *Wilson and Hey*'s [1995] rotational pole indicates that the spreading direction of the Nazca plate in the region is 186°. The exact orientation of the 91°W transform is difficult to measure, but linear ridges and troughs defined by bathymetric data (Figure 1; http://newport.pmel.noaa.gov/~chadwick/galapagos.html) and satellite gravity maps (http://topex.ucsd.edu/marine_ grav/mar_grav.html) strike 171°. Recent,

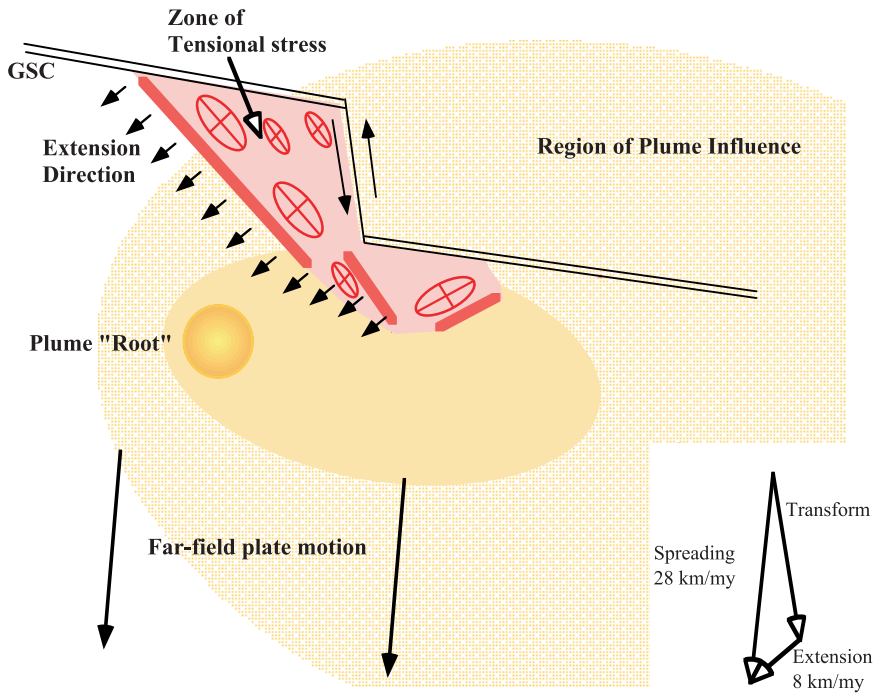

Figure 8. Conceptual model of the tectonic origin of the WDL. Orange tones indicate zone of influence of the Galápagos plume. Long arrows at the bottom of the figure oriented 186° show spreading direction of the Nazca plate. Short arrows represent extension necessary to accommodate plate spreading after strike-slip component of transform fault is removed. Bold red lines are observed volcanic lineaments (interpreted from bathymetric map, Figure 1). Ellipses are from the model of *Gudmundsson* [1995] for stresses around a transform fault–ridge intersection. Inset shows vector representation in velocity space of a model for strain partitioning through a combination of transform and extensional motions.

detailed bathymetric surveys of the northern Galápagos region confirm these observations (D. Christie, personal communication, 2002). Thus, the transform fault is oblique with respect to the spreading direction by 15° (Figure 8). We propose that spreading is accommodated by strain partitioning; slip along the transform at 171° is accompanied by diffuse southwestward extension across the entire inside corner of the 91°W transform (Figure 8). The 28 km/my half-spreading rate of the Nazca plate [*Demets et al.*, 1994] can be partitioned into 23.5 km/my strike-slip movement on the 91°W transform and 8.1 km/my of extension perpendicular to the WDL (Figure 8). Extension due to strain partitioning causes volcanism where it ordinarily would not occur across a broad zone between the ridge and the transform fault, distributed widely in space and time, and supplied by excess melt in the underlying mantle from the adjacent hot spot.

[37] Seismic evidence should provide a means of testing this hypothesis, but available data are sparse. The USGS NEIC database shows 2 epicenters (out of more than 100 regionally) near the WDL from 1973 to 2001. A compilation of hydrophone-determined T-phase epicenters shows no epicenters on the WDL between 1996 and 1999 (again, over 100 were determined regionally; http://www.pmel.noaa.gov/vents/acoustics/sosus.html).

[38] The Harvard Centroid Moment Tensor catalog lists six earthquakes in the vicinity of the 91°W transform. Five of these reflect strike-slip motion along the transform, with steeply dipping fault planes, an average strike of 176° ± 5°, left-lateral solutions, and an average magnitude of 5.4. The strike of the fault planes closely matches that determined by visual inspection of the bathymetry and confirms the oblique relationship between the transform and spreading direction. A sixth earth-

quake on 15 March 1982 has a normal solution with a fault plane that strikes 137° and dips 73° to the southwest. This is parallel to the WDL and provides evidence that extension accompanies the strike-slip faulting along this transform.

[39] Gravity data from the WDL are also consistent with extension along the lineament. *Feighner and Richards* [1995] previously suggested that the WDL is a lithospheric-scale fault. Their explanation for the fault, however, is that it forms the boundary between lithosphere in Airy compensation to the northeast and a continuous elastic plate to the southwest. In other words, their model does not include extension, but it was not considered and is probably not resolvable at the scale of their study.

[40] The geometric relationship between the WDL and the 91°W transform fault resembles that of an extensional transform zone (ETZs [*Taylor et al.*, 1994]). According to *Taylor et al.* [1994], ETZs "comprise overlapping volcanic systems and/or faults arranged in an en echelon pattern that form a neovolcanic/tectonic zone at angles between 15° and 45° to the spreading/rifting direction". Consistent with this definition, the strike of the 91°W transform makes an angle of 15° to the spreading direction of the Nazca plate. Moreover, the 145° strike of the WDL is oriented 40° to the spreading direction, well within the range reported by *Taylor et al.* [1994] for rifts associated with ETZs. Finally, the WDL has en echelon offsets at 1.1°N and at 1.5°N (Figure 1).

[41] The 91°W transform–WDL system is similar in many ways to the Tjørnes Fracture Zone north of Iceland. There, the main transform is the Husavik fault, which is oblique by 12° to the spreading direction. In the inside corner of the Kolbeinsey Ridge–Husavik Fault–Northern Volcanic Zone offset, there is a series of submarine en echelon volcanoes whose long axes are oriented approximately 40° to the Husavik fault [*Taylor et al.*, 1994], precisely the angle between the WDL and the 91° transform. Similarly, *Fujita and Sleep* [1978] note seamount chains along the Juan de Fuca ridge that are oriented similarly with respect to the ridge–transform intersections there.

[42] Another well-documented example of an oblique transform zone is Siqueiros, along the East Pacific Rise [*Pockalny et al.*, 1997]. There, the orientation of spreading rotated approximately 8° to the transform, causing transtension along the Siqueiros Fracture Zone. Unlike the WDL system, however, the Siqueiros transform appears to have accommodated the transtension by reorganizing into a series of intratransform spreading centers [*Pockalny et al.*, 1997]. At the WDL, transtension may be partitioned between strike-slip along the 91°W transform and broad extension across the WDL and the rest of the inside corner. Unlike the 91°W Galápagos and the Tjørnes transform systems, however, there is no mantle plume at the Siqueiros Fracture Zone. Thus, it appears that the creation of features like the WDL or the diagonally oriented volcanoes of the Tjørnes Fracture Zone require not only an active midocean ridge, but the combined effects of plume–ridge interaction. In the absence of an adjacent plume, transforms may simply reorient themselves in the direction of plate motion when subjected to oblique spreading stresses.

3.3. Geochemical Consequences of Diffuse Extension Over a Zone of Mixing

[43] In our model for the WDL, melts are produced along the lineament because of the combined effects of two magma sources, the plume and the ridge. The deviatoric tensional stress regime induced by the oblique 91°W transform and spreading permits magma ascent where it would not ordinarily occur and creates strongly elongate volcanic structures. Furthermore, extension may promote local mantle upwelling. The relatively thin lithosphere throughout the region [*Feighner and Richards*, 1995] is easily penetrated by melts, making it more likely that they will reach the surface than they would at locations farther south in the archipelago. The melts are derived from the local mantle immediately underlying each volcanic edifice, not from any type of channelized flow from the plume to the ridge.

[44] In contrast to the previous mechanisms proposed for the Wolf–Darwin Lineament, the extensional model is compatible with the majority of the

geological, geochemical, and geophysical observations described above. Because the magmatism is related to what is in essence a leaky zone of extension, there should be no major long-lived volcanic structures along the lineament. Moreover, the anomalously large, asymmetric seamounts (e.g., PL02-26 and 27) are aligned with the WDL, consistent with melt intrusion through a fissure. Similarly, volcanism along the lineament should be approximately contemporaneous and exhibit no age-progressive pattern, in agreement with existing observations [*White et al.*, 1993; *Sinton et al.*, 1996].

[45] Lavas from the northern WDL (Group I) appear to be derived from the same mantle source supplying the 91°–93°W segment of the GSC (Figure 7) [e.g., *Schilling et al.*, 1982; *Harpp and White*, 2001]. In contrast, lavas from the southern WDL (Group II) resemble those erupted along the GSC west of the 93°W propagator. Because the physical division between Groups I and II occurs near where the pseudofault from 93°W crosses the lineament, Group II seamounts are located on lithosphere that was originally produced west of 93°W at the GSC. The coincidence of the compositional boundary with the lithospheric discontinuity infers that WDL magmas are not the result of mantle flow either to or from the ridge. This also suggests that the compositional break formed in the mantle at the 93°W propagator is retained as the lithosphere is carried off axis.

[46] Helium isotope compositions belie these generalizations, however. The $^{3}He/^{4}He$ ratios of Group I lavas are similar to those of the GSC to the north, but the Group II lavas have higher $^{3}He/^{4}He$ ratios than GSC lavas to the west of 93°W [cf. *Graham et al.*, 1993; *Detrick et al.*, 2002]. Group I lavas therefore have slightly less plume-like helium signatures than Group II lavas, despite evidence to the contrary in other geochemical parameters (Figure 7). The plume component in the mantle underlying the WDL has a complex history, having been processed through the plume and also possibly the GSC magmatic system. Consequently, the helium isotopic ratios of WDL lavas may not directly reflect involvement of the plume in the mantle source. Similarly, helium appears to be decoupled from other isotopic and trace element tracers throughout the Galápagos region, a phenomenon that has been attributed to the extraction of helium by incipient melting within the plume before mixing with the asthenosphere [*Graham et al.*, 1993; *Kurz and Geist*, 1999].

[47] Whereas extensional transform zones are observed at spreading centers around the world [*Taylor et al.*, 1994], they are not marked by subaerial or submarine volcanic lineations such as the WDL unless there is a hot spot in proximity (e.g., Iceland). The generation of sufficiently large volumes of melt to construct the WDL is likely made possible by the serendipitous interaction of the adjacent and overlapping magmatic systems, the Galápagos plume and the GSC. Effectively, volcanism along the WDL may be thought of as a hybrid feature, the result of partial melting related to a spreading plume coupled with upwelling related to the midocean ridge. Both may be enhanced by extension. Indeed, preliminary interpretation of body wave tomography experiments by *Toomey et al.* [2001] indicates the presence of a zone of slow seismic velocities at shallow levels beneath the WDL.

3.4. Implications for Plume–Ridge Interaction

[48] Geochemical compositions indicate that the sources of the WDL lavas include contributions from the plume source, albeit to small and variable extents. The salient question, then, is whether the plume material in the WDL sources: a) originates directly from the plume; b) is a component of the regional return flow to the ridge; or c) is derived from previously plume-contaminated mantle that has already been processed through the GSC.

[49] The irregular distribution of plume material along the WDL, with differential contributions a mere 10 km apart, is inconsistent with a direct, constant supply of magma from the plume. Instead, such a distribution could result from small-scale eddies of plume material that become distributed in the mantle during return flow toward the ridge. Neither of these models, however, explains the

systematic geochemical differences between the northern and southern parts of the WDL (Groups I and II). If buoyant blobs of plume are rising through the mantle underlying the WDL, they may be directed toward the northern WDL by the lithospheric discontinuity created by the pseudofault near Wolf Island. Such a phenomenon could explain the peak of enrichment along the WDL at Wolf and Darwin Islands. Alternatively, plume material may be processed through the mantle that supplies the GSC prior to its transport to the WDL by shallow plate-driven flow. In this case, the geochemical discontinuity where the pseudofault intersects the WDL reflects greater plume contribution to the GSC east of the 93°W propagator, and this discontinuity in the mantle is maintained as the lithosphere is carried away from the ridge.

[50] Regardless of the precise mechanism, the fact that the WDL samples the underlying mantle passively provides a rare opportunity to observe the distribution of small-scale (5–10 km) heterogeneities throughout the asthenosphere. With more detailed sampling of the northern Galápagos region, it may be possible to address the issue of how plume material reaches the ridge in a more compelling way.

4. Conclusion

[51] The Wolf–Darwin lineament may not be the direct result of the Galápagos plume supplying the nearby Galápagos Spreading Center [e.g., *Morgan*, 1978]. Instead, we propose that the WDL merely reflects the regional stress field, because extension is occurring above part of the mantle that is unusually hot owing to the overlapping effects of midocean ridge magmatism and horizontal dispersal of a plume.

[52] Two circumstances conspire to cause a broad region of extension throughout the southwest corner of the 91°W transform. First, the stress regime within the inside corner of a ridge–transform intersection is strongly deviatoric [*Fujita and Sleep*, 1978; *Gudmundsson*, 1995], with the minimum principal stress direction essentially bisecting the ridge–transform intersection. The minimum principal stress then wraps around the outside corner at the other ridge–transform intersection until it is rotated 90°; this is exactly the orientation of Genovesa Ridge (Figures 1 and 8) [*Harpp et al.*, 2002]. The second effect is that the 91°W transform is transtensional, because the spreading direction is 15° clockwise of the strike of the transform.

[53] Migration of magma to the surface, then, is controlled by regional stress fields, resulting in constructional lineaments such as the WDL. According to this model, there should be no systematic distribution of volcanic ages within this magmatic province, as is observed [*White et al.*, 1993; *Sinton et al.*, 1996]. Similarly, this model predicts an irregular distribution of geochemical compositions throughout the northern Galápagos province. The individual volcanic centers are tapping mantle that is a spatially variable mixture of depleted mantle and plume material [e.g., *White et al.*, 1993], possibly a function of the amount of plume material supplied to each GSC segment.

[54] Our hypothesis can be tested by several methods. First, we predict that detailed seismic observation should detect epicenters in this region with focal mechanisms reflecting the state of stress predicted by mechanical models. Second, motion of Wolf and Darwin islands should be southwest with respect to the Nazca plate, which can be tested by geodetic measurements on those islands. Third, detailed sampling, age determinations, and geochemical analyses of all of the seamounts in the "inside corner" region near the 91°W transform fault should be performed to examine the two dimensional distribution of the mantle source components and melting conditions. Finally, similar volcanic alignments should be observed at other sites of plume–ridge interaction, where large-offset transforms create an unusually extensional near-ridge environment.

Acknowledgments

[55] This work has been generously supported by National Science Foundation grants CHE-9996141 and CHE-9996136 to Harpp and EAR-9612110 and EAR-0002818 to Geist. We are grateful to Bill White, Dave Graham, and Dave Christie for their detailed, constructive reviews and knowledge of the region. Thanks to Simon Kattenhorn for helpful discussions

and review. R. Wood and H. Tamarack provided helpful assistance during final preparation of the manuscript. Finally, we appreciate the proofreading efforts of Leslie Reed, Alison Koleszar, and John Chaklader. The authors contributed equally to this work.

References

Allan, J. F., R. Batiza, M. R. Perfit, D. J. Fornari, and R. O. Sack, Petrology of lavas from the Lamont seamount chain and adjacent East Pacific Rise, 10°N, *J. Petrol.*, *30*, 1245–1298, 1989.

Batiza, R., and D. Vanko, Volcanic development of small oceanic central volcanoes on the flanks of the East Pacific Rise inferred from narrow-beam echo-sounder surveys, *Mar. Geol.*, *54*, 53–90, 1983.

Canales, J. P., J. J. Danobeitia, R. S. Hooft, E. E. E. Detrick, R. Bartolome, and D. R. Naar, Variations in axial morphology along the Galápagos Spreading Center and the influence of the Galápagos hotspot, *J. Geophys. Res.*, *102*, 27,341–27,354, 1997.

Canales, J. P., G. Ito, R. S. Detrick, and J. Sinton, Compensation mechanism of the Galápagos swell, *Earth Planet. Sci. Lett.*, in press.

Christie, D. M., and C. Fox, Morphologic evolution of the margins of the Galápagos Platform, *Eos Trans. AGU*, *71*, 1578, 1990.

Christie, D. M., R. A. Duncan, A. R. McBirney, M. A. Richards, W. M. White, and K. S. Harpp, Drowned islands downstream from the Galápagos hotspot imply extended speciation times, *Nature*, *355*, 246–248, 1992.

Cullen, A. B., E. Vicenzi, and A. R. McBirney, Plagioclase-ultraphyric basalts of the Galápagos Archipelago, *J. Volcanol. Geotherm. Res.*, *37*, 325–337, 1989.

DeMets, C., R. G. Gordon, D. F. Argus, and S. Stein, Effect of recent revisions to the geomagnetic reversal time scale on estimate of current plate motions, *Geophys. Res. Lett.*, *21*, 2191–2194, 1994.

Detrick R. S., J. M. Sinton, G. Ito, J. P. Canales, M. Behn, T. Blacic, B. Cushman, J. E. Dixon, D. W. Graham, and J. J. Mahoney, Correlated geophysical, geochemical, and volcanological manifestations of plume-ridge interaction along the Galápagos Spreading Center, *Geochem. Geophys. Geosyst.*, *3*(10), 8501, doi:10.1029/2002GC000350, 2002.

Feighner, M. A., and M. A. Richards, Lithospheric structure and compensation mechanisms of the Galápagos Archipelago, *J. Geophys. Res.*, *99*, 6711–6729, 1995.

Fitton, J. G., A. D. Saunders, M. J. Norry, B. S. Hardarson, and R. N. Taylor, Thermal and chemical structure of the Iceland plume, *Earth Planet. Sci. Lett.*, *153*, 197–208, 1997.

Fornari, D. J., M. D. Kurz, D. J. Geist, P. D. Johnson, U. G. Peckman, and D. Scheirer, New perspectives on the structure and morphology of the submarine flanks of Galápagos volcanoes—Fernandina and Isabela, *Eos Trans. AGU*, 82, 2001.

Fujita, K., and N. H. Sleep, Membrane stresses near mid-ocean ridge–transform intersections, *Tectonophysics*, *50*, 207–221, 1978.

Geist, D. J., A. R. McBirney, and R. A. Duncan, Geology and petrology of lavas from San Cristobal Island, Galápagos Archipelago, *Geol. Soc. Am. Bull.*, *97*, 555–556, 1986.

Graham, D. W., D. M. Christie, K. S. Harpp, and J. E. Lupton, Mantle plume helium in submarine basalts from the Galápagos platform, *Science*, *262*, 2023–2026, 1993.

Gripp, A. E., and R. G. Gordon, Current plate velocities relative to hotspots incorporating the NUVEL-1 global plate model, *Geophys. Res. Lett.*, *17*, 1109–1112, 1990.

Gudmundsson, A., Stress fields associated with oceanic transform faults, *Earth Planet. Sci. Lett.*, *136*, 603–614, 1995.

Haase, K. M., and C. W. Devey, Geochemistry of lavas from the Ahu and Tupa volcanic fields, Easter Hotspot, southeast Pacific: Implications for intraplate magma genesis near a spreading axis, *Earth Planet. Sci. Lett.*, *137*, 129–143, 1996.

Haase, K. M., C. W. Devey, and S. L. Goldstein, Two-way exchange between the Easter mantle plume and the Easter microplate spreading axis, *Nature*, *382*, 344–346, 1996.

Haase, K. M., P. Stoffers, and C. D. Garbe-Schoenberg, The petrogenetic evolution of lavas from Easter Island and neighbouring seamounts, near-ridge hotspot volcanoes in the SE Pacific, *J. Petrol.*, *38*, 785–813, 1997.

Hanan, B. B., and J.-G. Schilling, Easter Microplate evolution: Pb isotope evidence, *J. Geophys. Res.*, *94*, 7432–7448, 1989.

Harpp K. S., and W. M. White, Tracing a mantle plume; isotopic and trace element variations of Galápagos seamounts, *Geochem. Geophys. Geosyst.*, *2*, paper number, doi:10.1029/2000GC000137, 2001.

Harpp, K. S., K. R. Wirth, and D. J. Korich, Northern Galápagos Province: Hotspot-induced, near-ridge volcanism at Genovesa Island, *Geology*, *30*, 399–402, 2002.

Kingsley, R., and J.-G. Schilling, Plume–ridge interaction in the Easter–Salas y Gomez seamount chain–Easter microplate system; Pb isotope evidence, *J. Geophys. Res.*, *103*, 24,159–24,177, 1998.

Kurz, M. D., and D. Geist, Dynamics of the Galápagos hotspot from helium isotope geochemistry, *Geochim. Cosmochim. Acta*, *63*, 4139–4156, 1999.

McBirney, A. R., and H. Williams, *Geology and Petrology of the Galápagos Islands*, *Geol. Soc. Am. Mem.*, vol. 118, 197 pp., 1969.

McDonough, W. F., and S. S. Sun, The composition of the Earth, *Chem. Geol.*, *120*, 223–253, 1995.

Morgan, W. J., Rodriguez, Darwin, Amsterdam . . ., a second type of hotspot island, *J. Geophys. Res.*, *83*, 5355–5360, 1978.

Pockalny, R. A., P. J. Fox, D. J. Fornari, K. C. Macdonald, and M. R. Perfit, Tectonic reconstruction of the Clipperton and Siqueiros fracture zones; Evidence and consequences of plate motion change for the last 3 Myr, *J. Geophys. Res.*, *102*, 3167–3181, 1997.

Pollard, D. D., and A. Aydin, Propagation and linkage of oceanic ridge segments, *J. Geophys. Res.*, *89*, 10,017–10,028, 1984.

Rappaport, Y., D. F. Naar, C. C. Barton, Z. J. Liu, and R. N. Hey, Morphology and distribution of seamounts surrounding Easter Island, *J. Geophys. Res.*, *102*, 24,713–24,728, 1997.

Schilling, J.-G., Fluxes and excess temperatures of mantle plumes inferred from their interaction with migrating mid-ocean ridges, *Nature*, *352*, 39–403, 1991.

Schilling, J.-G., R. N. Anderson, and P. Vogt, Rare earth Fe and Ti variations along the Galápagos spreading centre, and their relationship to the Galápagos mantle plume, *Nature*, *261*, 108–113, 1976.

Schilling, J.-G., R. H. Kingsley, and J. D. Devine, Galápagos hot spot–spreading center system, 1, Spatial petrological and geochemical variations (83°W–101°W), *J. Geophys. Res.*, *87*, 5593–5610, 1982.

Sinton, C. S., D. M. Christie, and R. A. Duncan, Geochronology of Galápagos seamounts, *J. Geophys. Res.*, *101*, 13,689–13,700, 1996.

Sinton, C. W., D. M. Christie, V. L. Coombs, R. L. Nielsen, and M. R. Fisk, Near-primary melt inclusions in anorthite phenocrysts from the Galápagos Platform, *Earth Planet. Sci. Lett.*, *119*, 527–537, 1993.

Small, C., Observations of ridge–hotspot interactions in the Southern Ocean, *J. Geophys. Res.*, *100*, 17,931–17,946, 1995.

Smith, D. K., and J. R. Cann, The role of seamount volcanism in crustal construction at the Mid-Atlantic Ridge (24°–30°N), *J. Geophys. Res.*, *97*, 1645–1658, 1992.

Standish, J., D. Geist, K. Harpp, and M. Kurz, The emergence of a Galápagos shield volcano, Roca Redonda, *Contrib. Mineral. Petrol.*, *133*, 136–148, 1998.

Taylor, B., K. A. W. Crook, and J. Sinton, Extensional transform zones and oblique spreading centers, *J. Geophys. Res.*, *99*, 1707–1719, 1994.

Toomey, D. R., E. E. E. Hooft, S. Solomon, D. James, and M. Hall, Upper mantle structure beneath the Galápagos Archipelago from body wave data, *Eos Trans. AGU*, *82*, F1205, 2001.

Verma, S. P., and J.-G. Schilling, Galápagos hot spot-spreading center system, 2, $^{87}Sr/^{86}Sr$ and large ion lithophile element variations (85°W–101°W), *J. Geophys. Res.*, *87*, 10,838–10,856, 1982.

Verma, S. P., J.-G. Schilling, and D. G. Waggoner, Neodymium isotopic evidence for Galápagos hotspot–spreading center system evolution, *Nature*, *306*, 654–657, 1983.

Vicenzi, E. P., A. R. McBirney, W. M. White, and M. Hamilton, The geology and geochemistry of Isla Marchena, Galápagos Archipelago: An ocean island adjacent to a mid-ocean ridge, *J. Volcanol. Geotherm. Res.*, *40*, 291–315, 1990.

White, W. M., A. R. McBirney, and R. A. Duncan, Petrology and geochemistry of the Galápagos Islands: Portrait of a pathological mantle plume, *J. Geophys. Res.*, *98*, 19,533–19,563, 1993.

Wilson, and Hey, History of rift propagation and magnetization intensity for the Cocos-Nazca spreading center, *J. Geophys. Res.*, *100*, 10,041–10,056, 1995.

Wolfe, C. J., I. T. Bjarnason, J. C. VanDecar, and S. C. Solomon, Seismic structure of the Iceland mantle plume, *Nature*, *385*, 245–247, 1997.

Yu, D., D. Fontignie, and J. G. Schilling, Mantle plume–ridge interactions in the central North Atlantic; A Nd isotope study of Mid-Atlantic Ridge basalts from 30°N to 50°N, *Earth Planet. Sci. Lett.*, *146*, 259–272, 1997.